Photon Blockade in Weakly Driven Cavity Quantum Electrodynamics Systems with Many Emitters

Rahul Trivedi,* Marina Radulaski, Kevin A. Fischer, Shanhui Fan, and Jelena Vučković
E. L. Ginzton Laboratory, Stanford University, Stanford, California 94305, USA

(Received 24 January 2019; published 21 June 2019)

We use the scattering matrix formalism to analyze photon blockade in coherently driven cavity quantum electrodynamics systems with a weak drive. By approximating the weak coherent drive by an input single- and two-photon Fock state, we reduce the computational complexity of the transmission and the two-photon correlation function from exponential to polynomial in the number of emitters. This enables us to easily analyze cavity-based systems containing ∼50 quantum emitters with modest computational resources. Using this approach we study the coherence statistics of photon blockade while increasing the number of emitters for resonant and detuned multiemitter cavity quantum electrodynamics systems—we find that increasing the number of emitters worsens photon blockade in resonant systems, and improves it in detuned systems. We also analyze the impact of inhomogeneous broadening in the emitter frequencies on the photon blockade through this system.

DOI: 10.1103/PhysRevLett.122.243602

Introduction.—Cavity quantum electrodynamics (CQED) is a fundamental model of light and matter which has been experimentally implemented in a variety of physical platforms. Atomic and solid state CQED systems with a few two-level emitters have exhibited a rich set of quantum phenomena in transmission statistics, including, but not limited to, the vacuum Rabi oscillations [1,2], the conventional and the unconventional photon blockade [3–5], and the photon-induced tunneling [6]. While suitable approximations can provide an understanding of the eigenstructure of multielement CQED systems [7,8] obtained in experiments [9,10], the numerical studies of light emission and scattering from this system have been limited due to the exponential scaling of the Hilbert space with the number of emitters.

The scattering matrix formalism for quantum-optical systems provides the solution to this problem. Recently, a general formalism for computing this scattering matrix for an arbitrary time-independent and time-dependent Markovian quantum-optical system was developed [11,12], reducing its computation to that of an effective propagator for the quantum-optical system. Use of the scattering matrices allows relating the transmission and two-photon correlation through a system to the single- and two-photon scattering matrix whose computation time scales as $\sim\mathcal{O}(N^3)$ and $\sim\mathcal{O}(N^6)$, respectively, in the number of emitters N.

In this Letter, we use the scattering matrix formalism to study multiemitter CQED systems with a large number of emitters ($N \sim 50$) driven by weak continuous-wave classical light (e.g., a laser). We show that increasing the number of emitters does not increase the depth of the photon blockade in resonant multiemitter CQED systems with identical emitters. However, find that increasing the number of emitters improves photon blockade if the emitters are detuned from the cavity resonance. Finally, we study the impact of inhomogeneous broadening [13–19] in the emitter frequencies on photon blockade in the multiemitter systems.

Simulation method.—A schematic of the considered system is shown in Fig. 1—a cavity, with annihilation operator a, is coupled to N two-level emitters, with lowering operators σ_i, $1 \le i \le N$. The cavity is excited through a waveguide, with a frequency-dependent annihilation operator b_ω, and the emission from the cavity is collected through another waveguide, with annihilation operator c_ω. The emitters, in addition to coupling to the cavity mode, also radiate into loss channels with annihilation operators $l_\omega^{(i)}$—these loss channels model the linewidths of the

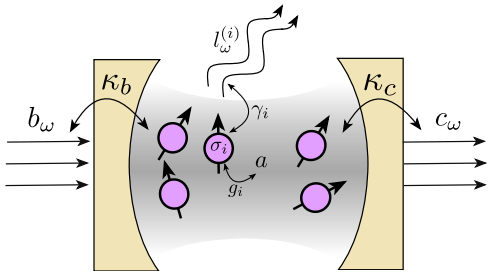

FIG. 1. Schematic of the multiemitter CQED system. An optical cavity mode couples to N emitters with coupling constants g_i, $1 \le i \le N$. The input and output coupling constants are κ_b and κ_c. In addition to the cavity, the emitters also couple to loss channels with coupling constants γ_i. The total decay rate of the cavity is given by $\kappa = \kappa_b + \kappa_c$ (we assume $\kappa_b = \kappa_c = \kappa/2$ throughout this Letter).

emitters. The Hamiltonian for the multiemitter CQED system is given by

$$H_{\rm sys} = \omega_c a^\dagger a + \sum_{i=1}^{N} [\omega_i \sigma_i^\dagger \sigma_i + g_i (a\sigma_i^\dagger + \sigma_i a^\dagger)], \quad (1)$$

where ω_c is the cavity resonance frequency, ω_i is the transition frequency of the ith emitter, and g_i is the coupling constant between the ith emitter and the cavity mode. We study the excitation of this system with a continuous-wave coherent state at frequency ω_L, described by an input state:

$$|\psi_{\rm in}\rangle = \exp[\beta_0 (b_{\omega_L}^\dagger - b_{\omega_L})]|{\rm vac}\rangle, \quad (2)$$

where β_0^2 is the photon flux (number of photons per unit time) in the coherent state. As is detailed in the Supplemental Material [20], we establish the following relationship of the transmission $T(\omega_L)$ and two-photon correlation $g^{(2)}(t_1, t_2; \omega_L)$ to the single-photon $[S_c(\cdot)]$ and two-photon $[S_{c,c}(\cdot)]$ scattering matrices for continuous-wave input in the limit of small input photon flux β_0^2:

$$T(\omega_L) = \left| \int_{t'=-\infty}^{\infty} S_c(t;t') \exp(-i\omega_L t') dt' \right|^2 \quad (3a)$$

$$g^{(2)}(t_1, t_2; \omega_L) = \frac{1}{4T^2(\omega_L)} \times \left| \int_{t_1', t_2'=-\infty}^{\infty} S_{c,c}(t_1, t_2; t_1', t_2') \exp[-i\omega_L (t_1' + t_2')] dt_1' dt_2' \right|^2, \quad (3b)$$

where the S matrices capture scattering of photons propagating in the input waveguide (with annihilation operator b_ω) to the output waveguide (with annihilation operator c_ω). The scattering matrices are functions only of the system operators and external coupling constants $\kappa_{b,c}$ and γ_n.

The dominant cost for computing these scattering matrices is that of diagonalizing the effective Hamiltonian $H_{\rm eff}$ [20]:

$$H_{\rm eff} = H_{\rm sys} - \frac{i\kappa}{2} a^\dagger a - \sum_{n=1}^{N} \frac{i\gamma_n}{2} \sigma_n^\dagger \sigma_n, \quad (4)$$

where $\kappa = \kappa_b + \kappa_c$ is the total decay rate for the optical cavity. Since $H_{\rm eff}$ conserves the total excitation number $(a^\dagger a + \sum_{n=1}^{N} \sigma_n^\dagger \sigma_n)$, this diagonalization can be performed separately within the excitation conserving subspaces of the full Hilbert space. When computing the single- and two-photon scattering matrices, it is only necessary to diagonalize the effective Hamiltonian within the single- and two-excitation subspaces the cost of which is $\sim\mathcal{O}(N^3)$ and $\sim\mathcal{O}(N^6)$, respectively. We note that when the emitters are identical (i.e., $\omega_i = \omega$, $\gamma_i = \gamma$, and $g_i = g$ for all $i \in \{1, 2, \ldots, N\}$), by utilizing the Clebsch-Gordan series this diagonalization can be mapped to the diagonalization of 3×3 and 2×2 complex matrices [20].

Having diagonalized $H_{\rm eff}$, the transmission $T(\omega_L)$ and equal-time two-photon correlation $g^{(2)}(0;\omega_L) = g^{(2)}(t,t;\omega_L)$ can be expressed as [20]

$$T(\omega_L) = \kappa_b \kappa_c \left| \sum_{i=1}^{\mathcal{N}_1} \frac{(\langle {\rm G}|a|\phi_i^{(1)}\rangle_{\rm T})^2}{\lambda_i^{(1)} - \omega_L} \right|^2, \quad (5a)$$

$$g^{(2)}(0;\omega_L) = \left| \sum_{i=1}^{\mathcal{N}_2} \Gamma_i(\omega_L) \right|^2, \quad (5b)$$

where $|{\rm G}\rangle$ is the ground state of the multiemitter CQED system, $\langle\cdot\rangle_T$ denotes a "transpose" inner product between two states, $\mathcal{N}_i$ is the dimensionality of the ith excitation subspace of the multiemitter CQED system, $(\lambda_j^{(i)}, |\phi_j^{(i)}\rangle)$ are the eigenvalues and eigenstates of $H_{\rm eff}$ within the ith excitation subspace and $\Gamma_i(\omega_L)$, given below, can be interpreted as the contribution of the ith two-excitation eigenstate to the equal-time two-photon emission:

$$\Gamma_i(\omega_L) = \frac{\kappa_b \kappa_c}{T(\omega_L)} \left(\frac{\langle {\rm G}|a^2|\phi_i^{(2)}\rangle_T}{\lambda_i^{(2)} - 2\omega_L} \right) \times \sum_{j=1}^{\mathcal{N}_1} \left(\frac{\langle \phi_i^{(2)}|a^\dagger|\phi_j^{(1)}\rangle_T \langle \phi_j^{(1)}|a^\dagger|{\rm G}\rangle_T}{\lambda_j^{(1)} - \omega_L} \right). \quad (6)$$

These expressions for $T(\omega_L)$ and $g^{(2)}(0;\omega_L)$ explicitly show their dependence on the energy eigenvalues $[\sim{\rm Re}(\lambda_i^{(j)})]$, linewidths $[\sim{\rm Im}(\lambda_i^{(j)})]$, as well as the eigenstates $(|\phi_j^{(i)}\rangle)$ of the multiemitter CQED systems.

Results.—Using a large number of identical emitters coupling coherently to the same cavity mode is a potential strategy to achieve strong coupling between the emitters and the cavity in a situation where an individual emitter only weakly couples to the cavity mode. Figures 2(a)–2(b) show the transmissivity $T(\omega_L)$ and equal-time correlation $g^{(2)}(0;\omega_L)$ for multiemitter CQED systems with 1–100 emitters. Consistent with the result obtained on a direct diagonalization of $H_{\rm sys}$, we observe that the splitting between the polaritonic peaks in the transmissivity scales as $\sqrt{N}$. We also observe that the minimum two-photon correlation $g^{(2)}(0;\omega_L)$, which is achieved at the polaritonic frequencies, tends towards unity with an increase in the number of emitters for both strongly coupled emitters [Fig. 2(a)] and weakly coupled emitters [Fig. 2(b)]. This

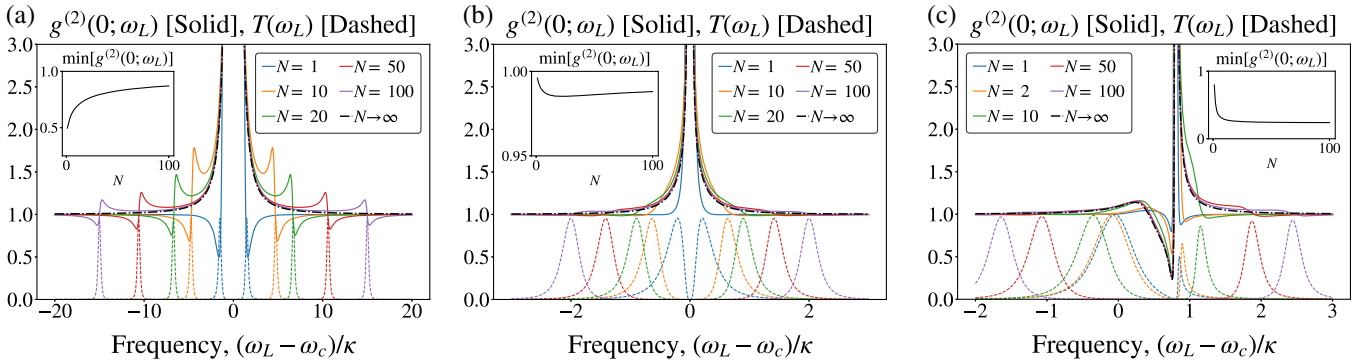

FIG. 2. Equal-time correlation $g^{(2)}(0;\omega_L)$ and transmissivity $T(\omega_L)$ for (a) strongly coupled resonant emitters ($g=2\kappa, \omega_e=\omega_c$), (b) weakly coupled resonant emitters ($g=0.2\kappa, \omega_e=\omega_c$), and (c) weakly coupled detuned emitters ($g=0.2\kappa, \omega_e-\omega_c=0.8\kappa$). The insets show the dependence of $\min_{\omega_L}[g^{(2)}(0;\omega_L)]$ as a function of N and the dashed lines show $\lim_{N\to\infty} g^{(2)}(0;\omega_L)$ computed using Eq. (8). Increasing the number of emitters clearly deteriorates the polaritonic photon blockade observed in the system. For detuned systems, increasing the number of emitters enhances the interference-based blockade. $\gamma=0.01\kappa$ is assumed in all simulations.

trend can be easily explained by looking closely at the "anharmonicity" ($\delta\omega_{1,2}$) between the single- and two-excitation eigenenergies of the multiemitter CQED system:

$$\Delta\omega_{1,2}=\min_{i,j}|\mathrm{Re}[2\lambda_i^{(1)}]-\mathrm{Re}[\lambda_j^{(2)}]|. \tag{7}$$

Figure 3(a) shows $\Delta\omega_{1,2}$ as a function of N along with the linewidth $\delta\omega_2=\mathrm{Im}[2\lambda_i^{(2)}]$ of the most harmonic eigenstate in the two-excitation subspace—increasing the number of emitters makes the system's energy levels more equally spaced while saturating their linewidths, thereby worsening photon blockade. It is worth noting that with the weakly coupled emitters the value of the $\min[g^{(2)}(0;\omega_L)]$ has an initial decrease, before monotonically increasing with the number of emitters consistent with previously reported results [8]. We also observe a pronounced "bunching" peak in $g^{(2)}(0;\omega_L)$ for strongly coupled emitters [Fig. 2(a)], near the antibunching dip—this corresponds to $2\omega_L$ being resonant with the two-excitation eigenstates. $g^{(2)}(0;\omega_L)$ at the bunching peak also tends to 1 as $N\to\infty$ due to the system eigenstates becoming increasingly harmonic. Moreover, $g^{(2)}(0;\omega_L)$ can be analytically evaluated in the limit of $N\to\infty$ to obtain [20]

$$\lim_{N\to\infty} g^{(2)}(0;\omega_L)=\left|1-\frac{g^2}{(\omega_L-\lambda_e)(2\omega_L-\lambda_e-\lambda_c)}\right|^2, \tag{8}$$

where $\lambda_e=\omega_e-i\gamma/2$ and $\lambda_c=\omega_c-i\kappa/2$. As can be seen from Figs. 2(a) and 2(b), in the limit of large number of emitters, the multiemitter system does not show any blockade—photon bunching can be seen at $\omega_L\sim\omega_c$ as a consequence of near zero single-photon transmission.

We next study the impact of detuning between the emitters and the optical mode on the polaritonic photon blockade [Fig. 2(c)]. Consider the transmission line shape: there is a distinct Fano dip to nearly zero transmission at $\omega_L\approx\omega_e$ where the single-photon transmission through the two single-excitation eigenstates (one being more cavity-like and the other being more emitterlike) exactly cancels. Towards the right of this Fano dip, the light antibunches [$g^{(2)}(0;\omega_L)<1$] owing to the standard polaritonic photon blockade of a detuned system [25,26]. Because of the multiemitter system becoming more harmonic with an increase in the number of emitters [Fig. 3(a)], this blockade effect degrades similar to that in the resonant CQED system. Photon bunching [$g^{(2)}(0;\omega_L)>1$] is observed exactly at the Fano dip due to the single-photon transmission becoming nearly zero—within the framework of scattering theory, this is equivalent to the contribution of the unconnected (linear or frequency preserving) part of the scattering matrix being small in the output state, and the scattering happening almost entirely from the connected (nonlinear or frequency mixing) part of the two-photon S matrix [27].

Slightly left of the Fano dip, we again observe photon antibunching—moreover, unlike polaritonic blockade, the blockade depth increases with increasing N. This blockade occurs due to a destructive interference between the two-photon emissions from different two-excitation eigenstates. More insight into this phenomenon can be obtained by closely studying the two-excitation eigenstates as well as their contribution to two-photon emission. Note from Eqs. (5b) and (6) that only the two-excitation eigenstates which have nonzero overlap with two photons in the cavity (i.e., $\langle \mathrm{G}|a^2|\phi_i^{(2)}\rangle\neq 0$) have a nonzero contribution to $g^{(2)}(0)$. When all the emitters are identical, there are three such two-excitation eigenstates—$|\phi_\pm^{(2)}\rangle$ which have a probability of $1/4$ of having two photons in the cavity in the limit of $N\to\infty$, and $|\phi_0^{(2)}\rangle$ which when $N\to\infty$ has a probability of $1/2$ of having two photons in the cavity [20]. Figures 3(b)–3(c) show the amplitude and phase of the

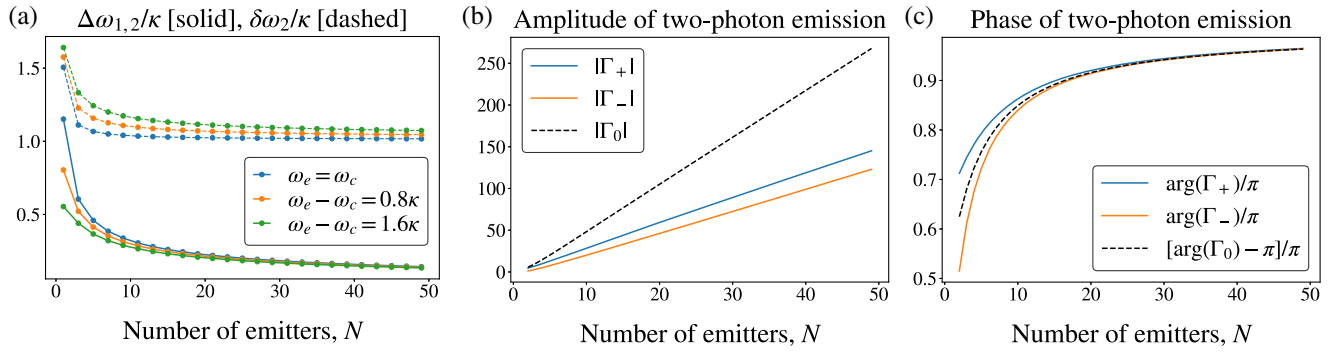

FIG. 3. (a) Anharmonicity $\Delta\omega_{1,2}$ and the linewidth $\delta\omega_2$ of the most harmonic eigenstate in the second excitation subspace as a function of number of emitters. We have used $g = 2\kappa$ and only considered those two-excitation eigenstates which have a nonzero overlap with two photons in the cavity while computing $\Delta\omega_{1,2}$ and $\delta\omega_2$. (b) Amplitude and phase of the equal-time two-photon emission $(\Gamma_\pm, \Gamma_0)$ from the three eigenstates $(|\phi_\pm^{(2)}\rangle, |\phi_0^{(2)}\rangle)$ that contribute to $g^{(2)}(0;\omega_L)$ in a detuned multiemitter CQED system with weakly coupled emitters ($g = 0.2\kappa$, $\omega_e - \omega_c = 0.8\kappa$) at the frequency corresponding to the interference-based blockade. $\gamma = 0.01\kappa$ is assumed in all simulations.

contribution of these three eigenstates to equal-time two-photon emission [i.e., $\Gamma_i(\omega_L)$ defined by Eq. (6)] at the blockade frequency—it can easily be seen that individually the eigenstates have significant two-photon emission, with the amplitude of emission being proportional to the probability of the eigenstate having two photons in the cavity mode. However, the two-photon emission from $|\phi_0^{(2)}\rangle$ is out of phase from the emission of $|\phi_\pm^{(2)}\rangle$, with the phase difference between them approaching π as the number of emitters increases. This explains the interference-based character of this blockade, as well as its dependence on N. The limit of $g^{(2)}(0;\omega_L)$ as $N \to \infty$, given by Eq. (8) and plotted in Fig. 2(c), also shows a pronounced interference-based antibunching, along with a disappearance of the polaritonic blockade. Moreover, the interference-based blockade can be made deeper by increasing the detuning between the emitters and the cavity mode [20]. We also note that the transmission $T(\omega_L)$ at the

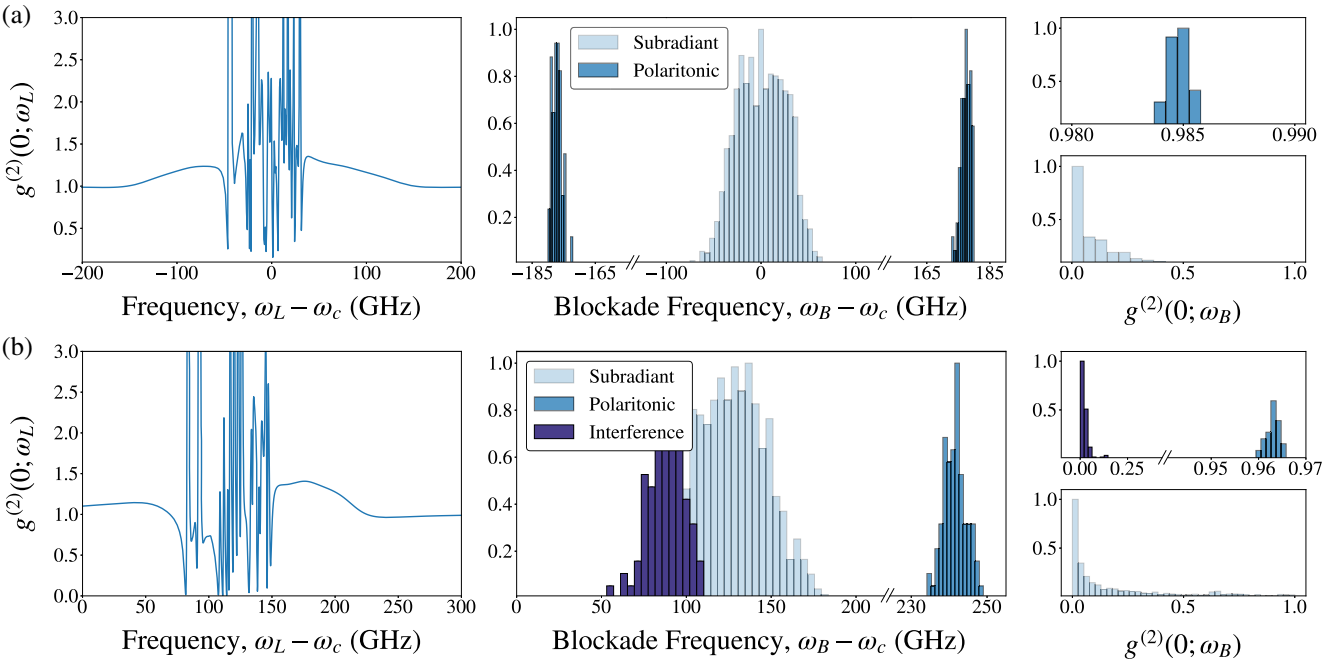

FIG. 4. Impact of inhomogeneous broadening on the photon blockade in multiemitter CQED systems for (a) the emitters, on an average, being resonant with the cavity. (b) emitters that are, on an average, detuned from the cavity resonance by $\langle\omega_e\rangle - \omega_c = 0.8\kappa = 2\pi \times 20$ GHz. For both cases, we show a typical line shape $g^{(2)}(0;\omega_L)$, and the statistics of the frequencies ω_B and the $g^{(2)}(0;\omega_B)$ values for the polaritonic and subradiant photon blockade (note that the y axis in the histogram is the unnormalized frequency of occurrence of the sample statistic). Parameter values $\Delta = 25$ GHz, $\kappa = 2\pi \times 25$ GHz, $g = 0.2\kappa = 2\pi \times 5$ GHz, and $\gamma = 2\pi \times 0.3$ GHz are assumed in all simulations.

interference-based photon blockade is small—it scales in inverse proportion to N^2 [20]—there thus exists a trade-off between the purity of the single-photon state emitted by these systems and the brightness of the single-photon state.

While the previous analysis was primarily done under the assumption of identical emitters, emitters in practical systems are inhomogeneously broadened; i.e., they have slightly different transition frequencies. For solid-state color centers, the distribution of the emitter frequencies can be modeled as a normal distribution with standard deviation $\Delta \lesssim 20$ GHz [16,18,19]. Results of a Monte Carlo analysis on the transmission and equal-time two-photon correlation through the multiemitter system are shown in Fig. 4(a) for resonant emitters and Fig. 4(b) for detuned emitters. We observe an emergence of a large number of very narrow linewidth dips in $g^{(2)}(0;\omega_L)$ which correspond to the subradiant photon blockade that has been studied in CQED systems with two nonidentical emitters [28]. The occurrence of these dips is due to subradiant states. These highly entangled states that did not overlap with the cavity mode when the emitters were identical, now do overlap with the cavity mode and hence contribute to light emission from the system. These blockades reach very low $g^{(2)}(0;\omega_L)$ values even for emitters that individually couple to the cavity only weakly. Moreover, for the resonant system, the distribution of the frequencies of the blockade dips (ω_B) reveal that the spread in the frequencies of the subradiant photon blockade is of the order of the inhomogeneous broadening in the emitter frequencies, whereas the frequencies of polaritonic photon blockade are significantly more robust to inhomogeneous broadening in the emitter frequencies albeit with a much larger value of $g^{(2)}(0;\omega_B)$. A similar trend is observed in the detuned system [Fig. 4(b)], with the polaritonic dip being robust to inhomogeneous broadening, and the interference-based dips (identified as the first dip which smoothly plateaus to 1 as $|\omega_L| \to \infty$) are much more sensitive to the inhomogeneous broadening while reaching very low $g^{(2)}(0;\omega_B)$ values (∼0–0.1) similar to the identical-emitter system.

Finally, our study has uncovered two fundamental trade-offs in multiemitter CQED systems which can help inform future experiments and their suitability for quantum information processing applications. First, for a given emitter-cavity coupling strength and cavity decay rate, there exists a trade-off between the achievable transmission and the depth of photon blockade [measured as $g^{(2)}(0;\omega_B)$]. Increasing either the cavity-emitter detuning or the number of emitters increases the depth of photon blockade, but also reduces transmission at the blockade frequency. Second, a trade-off exists between the depth of achievable blockade and robustness of the blockade frequency to inhomogeneous broadening—polaritonic photon blockade, which typically has $g^{(2)}(0;\omega_B) \sim 1$, is robust to inhomogeneous broadening, while detuning the emitters from the cavity resonance can allow the multiemitter CQED system to exhibit the interference-based photon blockade with significantly lower $g^{(2)}(0;\omega_L)$. However, relying on destructive interference of two-photon emissions from various two-excitation eigenstates makes the blockade sensitive to the emitter frequencies. Moreover, the subradiant dips in the photon blockade also provide very low $g^{(2)}(0;\omega_B)$, but the blockade frequencies ω_B are difficult to engineer without precise control over the emitter frequencies.

We thank Shuo Sun and Daniil Lukin for fruitful discussions. We gratefully acknowledge financial support from the Air Force Office of Scientific Research (AFOSR) MURI Center for Attojoule Optoelectronics Award No. FA9550-17-1-0002. R. T. acknowledges support from Kailath Stanford Graduate Fellowship. M. R. acknowledges support from Nano- and Quantum Science and Engineering Postdoctoral Fellowship at Stanford University.

*rtrivedi@stanford.edu

[1] M. Brune, F. Schmidt-Kaler, A. Maali, J. Dreyer, E. Hagley, J. M. Raimond, and S. Haroche, Quantum Rabi Oscillation: A Direct Test of Field Quantization in a Cavity, Phys. Rev. Lett. **76**, 1800 (1996).

[2] T. Yoshie, A. Scherer, J. Hendrickson, G. Khitrova, H. M. Gibbs, G. Rupper, C. Ell, O. B. Shchekin, and D. G. Deppe, Vacuum Rabi splitting with a single quantum dot in a photonic crystal nanocavity, Nature (London) **432**, 200 (2004).

[3] K. M. Birnbaum, A. Boca, R. Miller, A. D. Boozer, T. E. Northup, and H. J. Kimble, Photon blockade in an optical cavity with one trapped atom, Nature (London) **436**, 87 (2005).

[4] A. Imamoglu, H. Schmidt, G. Woods, and M. Deutsch, Strongly Interacting photons in a Nonlinear Cavity, [Phys. Rev. Lett. **79**, 1467 (1997)]; Erratum, Phys. Rev. Lett.**81**, 2836(E) (1998).

[5] H. J. Snijders, J. A. Frey, J. Norman, H. Flayac, V. Savona, A. C. Gossard, J. E. Bowers, M. P. van Exter, D. Bouwmeester, and W. Löffler, Observation of the Unconventional Photon Blockade, Phys. Rev. Lett. **121**, 043601 (2018).

[6] A. Faraon, I. Fushman, D. Englund, N. Stoltz, P. Petroff, and J. Vučković, Coherent generation of non-classical light on a chip via photon-induced tunnelling and blockade, Nat. Phys. **4**, 859 (2008).

[7] I. Diniz, S. Portolan, R. Ferreira, J. M. Gérard, P. Bertet, and A. Auffeves, Strongly coupling a cavity to inhomogeneous ensembles of emitters: Potential for long-lived solid-state quantum memories, Phys. Rev. A **84**, 063810 (2011).

[8] M. Radulaski, K. A. Fischer, and J. Vučković, Nonclassical light generation from iii–v and group-iv solid-state cavity quantum systems, in *Advances In Atomic, Molecular, and Optical Physics* (Elsevier, New York, 2017), Vol. 66, pp. 111–179.

[9] R. J. Thompson, G. Rempe, and H. J. Kimble, Observation of Normal-Mode Splitting for an Atom in an Optical Cavity, Phys. Rev. Lett. **68**, 1132 (1992).

[10] T. Zhong, J. M. Kindem, J. Rochman, and A. Faraon, Interfacing broadband photonic qubits to on-chip cavity-protected rare-earth ensembles, Nat. Commun. **8**, 14107 (2017).

[11] S. Xu and S. Fan, Input-output formalism for few-photon transport: A systematic treatment beyond two photons, Phys. Rev. A **91**, 043845 (2015).

[12] R. Trivedi, K. Fischer, S. Xu, S. Fan, and J. Vuckovic, Few-photon scattering and emission from low-dimensional quantum systems, Phys. Rev. B **98**, 144112 (2018).

[13] R. E. Evans, A. Sipahigil, D. D. Sukachev, A. S. Zibrov, and M. D. Lukin, Narrow-linewidth homogeneous optical emitters in diamond nanostructures via silicon ion implantation, Phys. Rev. Applied **5**, 044010 (2016).

[14] J. L. Zhang, S. Sun, M. J. Burek, C. Dory, Y.-K. Tzeng, K. A. Fischer, Y. Kelaita, K. G. Lagoudakis, M. Radulaski, Z.-X. Shen *et al.*, Strongly cavity-enhanced spontaneous emission from silicon-vacancy centers in diamond, Nano Lett. **18**, 1360 (2018).

[15] C. Dory, D. Vercruysse, K. Y. Yang, N. V. Sapra, A. E. Rugar, S. Sun, D. M. Lukin, A. Y. Piggott, J. L. Zhang, M. Radulaski *et al.*, Optimized diamond quantum photonics, arXiv:1812.02287.

[16] M. Radulaski, M. Widmann, M. Niethammer, J. L. Zhang, S.-Y. Lee, T. Rendler, K. G. Lagoudakis, N. T. Son, E. Janzen, T. Ohshima *et al.*, Scalable quantum photonics with single color centers in silicon carbide, Nano Lett. **17**, 1782 (2017).

[17] D. O. Bracher, X. Zhang, and E. L. Hu, Selective Purcell enhancement of two closely linked zero-phonon transitions of a silicon carbide color center, Proc. Natl. Acad. Sci. U.S.A. **114**, 4060 (2017).

[18] H. B. Banks, O. O. Soykal, R. Myers-Ward, D. K. Gaskill, T. L. Reinecke, and S. G. Carter, Resonant optical spin initialization and readout of single silicon vacancies in 4H-SiC, Phys. Rev. Applied **11**, 024013 (2019).

[19] D. Lukin, C. Dory, M. Radulaski, S. Sun, D. Vercruysse, and J. Vuckovic, , *4H-SiC-on-Insulator Platform for Quantum Photonics with Color Centers* (American Physical Society, College Park, MD, 2019).

[20] See Supplemental Material at http://link.aps.org/supplemental/10.1103/PhysRevLett.122.243602 for details on explicit computation of $T(\omega_L)$ and $g^{(2)}(t_1, t_2; \omega_L)$ using the scattering matrix formalism, efficient diagonalization of H_{eff} when the emitters are identical, derivation of Eqs. (5), (6), and (8) and the impact of system parameters on $\lim_{N\to\infty} g^{(2)}(0; \omega_L)$, which includes Refs. [21–24].

[21] J. R. Johansson, P. D. Nation, and F. Nori, QuTIP: An open-source Python framework for the dynamics of open quantum systems, Comput. Phys. Commun. **183**, 1760 (2012).

[22] M. Tavis and F. W. Cummings, Exact solution for an n-molecule-radiation-field Hamiltonian, Phys. Rev. **170**, 379 (1968).

[23] M. Tavis and F. W. Cummings, Approximate solutions for an n-molecule-radiation-field Hamiltonian, Phys. Rev. **188**, 692 (1969).

[24] R. H. Dicke, Coherence in spontaneous radiation processes, Phys. Rev. **93**, 99 (1954).

[25] F. P. Laussy, E. del Valle, M. Schrapp, A. Laucht, and J. J. Finley, Climbing the Jaynes-Cummings ladder by photon counting, J. Nanophoton. **6**, 061803 (2012).

[26] K. Müller, A. Rundquist, K. A. Fischer, T. Sarmiento, K. G. Lagoudakis, Y. A. Kelaita, C. S. Muñoz, E. del Valle, F. P. Laussy, and J. Vučković, Coherent Generation of Nonclassical Light on Chip Via Detuned Photon Blockade, Phys. Rev. Lett. **114**, 233601 (2015).

[27] J.-T. Shen and S. Fan, Strongly Correlated Two-Photon Transport in a One-Dimensional Waveguide Coupled to a Two-Level System, Phys. Rev. Lett. **98**, 153003 (2007).

[28] M. Radulaski, K. A. Fischer, K. G. Lagoudakis, J. L. Zhang, and J. Vučković, Photon blockade in two-emitter-cavity systems, Phys. Rev. A **96**, 011801(R) (2017).